Supporting Information

Ultrafast Charge Transfer Through Non-Covalent Au-N Interactions in Molecular Systems

Gregor Kladnik[a,c,1], Dean Cvetko[a,c,1,2], Arunabh Batra[b], Martina Dell'Angela[c,d], Albano Cossaro[c], Maria Kamenetska[b], Latha Venkataraman[b,2], Alberto Morgante[c,d]

[a]*Department of Physics, University of Ljubljana, Ljubljana, Slovenia*
[b]*Department of Applied Physics and Applied Mathematics, Columbia University, New York, NY*
[c]*CNR-IOM Laboratorio Nazionale TASC, Basovizza SS-14, km 163.5, I-34012 Trieste, Italy*
[d]*Department of Physics, University of Trieste, Trieste, Italy*

[1]These authors contributed equally to this work
[2]Corresponding Authors: (DC) dean.cvetko@fmf.uni-lj.si, (LV) lv2117@columbia.edu

Contents

Supporting Figures:

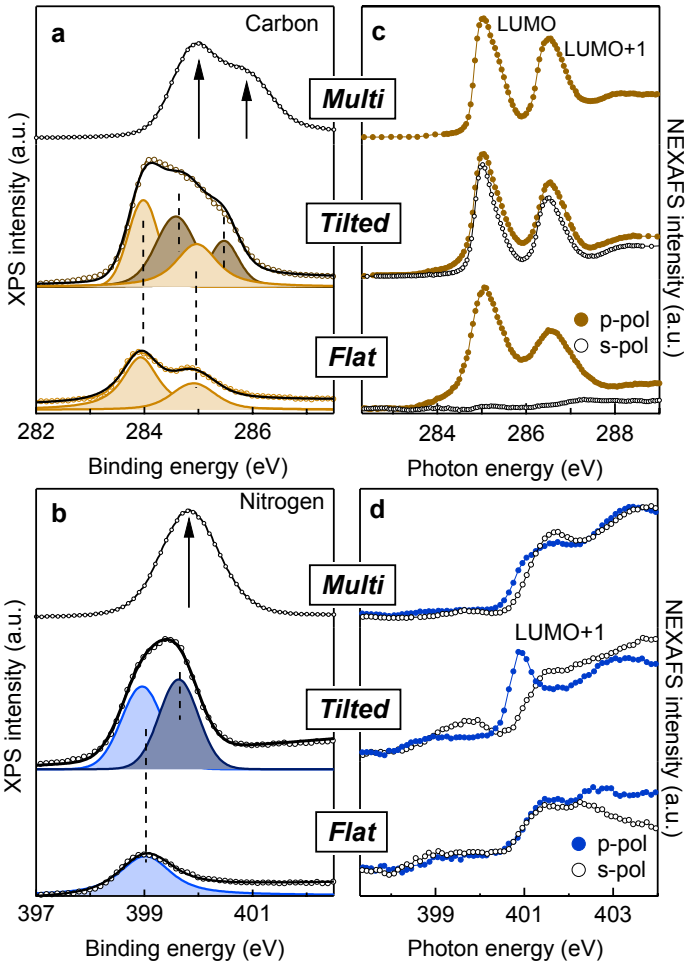

Fig. S1. XPS of (a) carbon 1s and (b) nitrogen 1s for multi, tilted and flat BDA phases on Au. NEXAFS at the (c) carbon K-edge and (d) nitrogen K-edge with the photon polarization parallel (p-pol) or perpendicular (s-pol) to the surface normal.

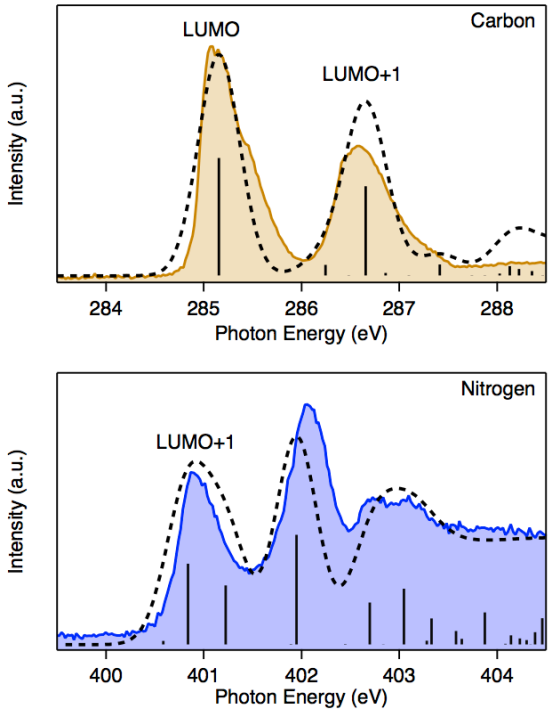

Fig. S2. Calculated and measured NEXAFS spectra for carbon and nitrogen spectra where sticks indicate calculated transition energies, which are broadened with a 0.5 eV FWHM Gaussian to yield the dashed curves. Experimental curves are shown in shaded brown (C) and blue (N).

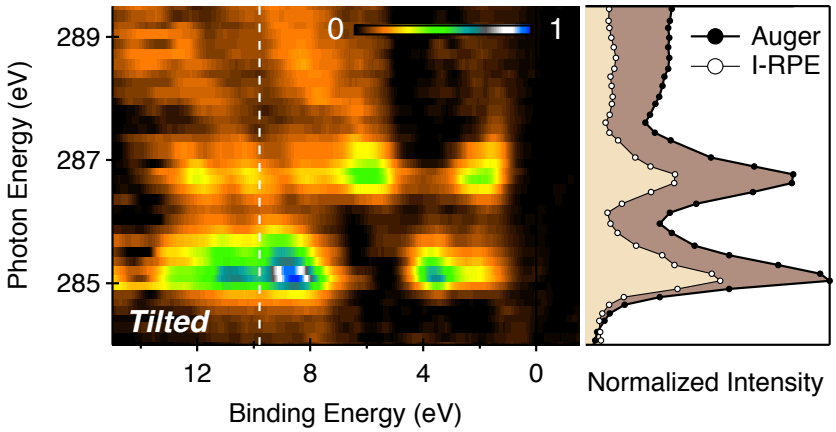

Fig. S3. Carbon K-edge resonant photoemission (RPES) on *tilted* phase. The 2D intensity maps represent normalized resonant intensity due to participator decay processes. The right panel shows the respective Auger intensity and integrated resonant intensity (I-RPE) across the main C K-edge resonances (LUMO and LUMO+1). The dotted white line on the RPES maps indicate the high binding energy cutoff for I-RPE integration

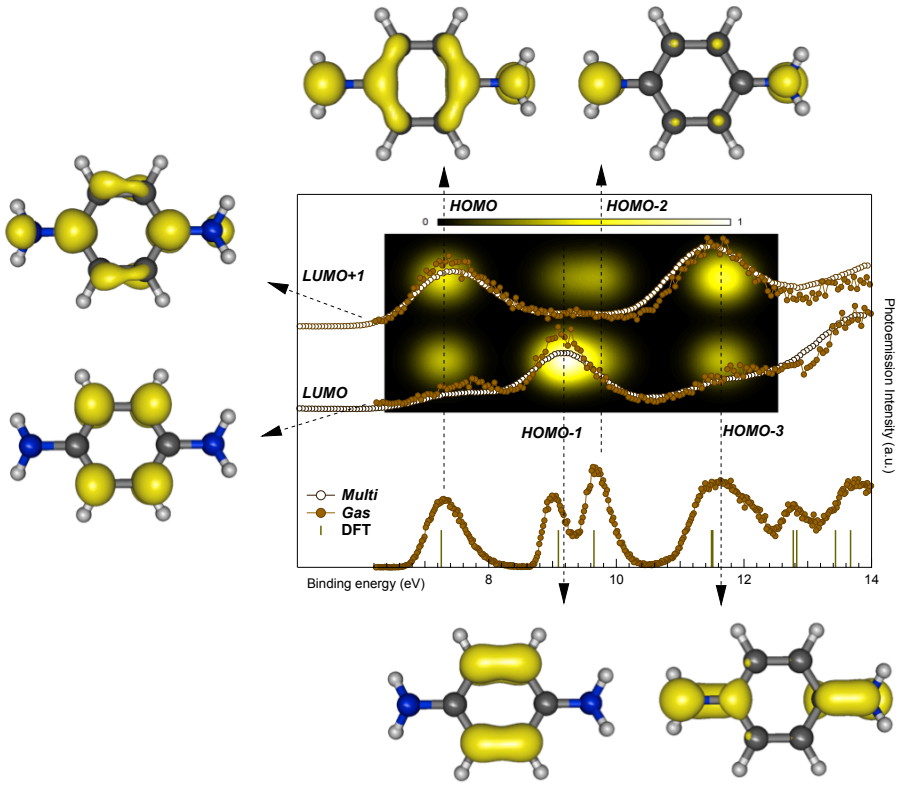

Fig. S4. RPES spectra at C1s to LUMO (hv=285.1 eV, top) and C1s to LUMO+1 (hv =286.8 eV, middle) absorption lines measured in gas phase (filled circles) and *multi* (empty circles). High-resolution gas phase valence band spectrum with hv =90 eV is also shown (bottom curve). The vertical bars indicate DFT calculated energy levels. Corresponding calculated orbitals of the BDA molecule are also shown. The calculated transfer integral representing the strength of valence band resonances that involve particular HOMO and LUMO pairs is shown in a 2D intensity map, with greater intensity representing greater orbital overlap.

X-ray Photoemission Spectroscopy Measurements

X-ray photoemission spectroscopy (XPS) measurements were performed at the ALOISA beamline[1] with the x-ray beam at grazing-incidence (4^o) to the sample and with the electric field perpendicular to the sample (p-pol). Photoelectrons from the sample were collected normal to the surface using a hemispherical electron analyzer with an acceptance angle of 2^o, and overall energy resolution of ~ 0.2 eV. The energy scale for XPS spectra was calibrated by aligning the Au $4f_{7/2}$ peak to a binding energy of 84.0 eV, or where identified, aligning the Fermi energy to zero.

Fig. S1a shows C1s XPS measurements for three different phases, *multi*, *tilted* and *flat* (top to bottom) with incident photon energy of 400 eV. Two principal C1s components (at 285.0 and 285.9 eV) are seen in *multi,* corresponding to emission from the $C_{1,4}$ and $C_{2,3,4,5}$ carbon sites respectively (Figure 1). For the *flat* phase, this doublet is shifted by ~1 eV to lower binding energies due to screening effects from the Au[2,3]. Such a shift is typical for molecules adsorbed on metal surfaces and reflects molecular distances ~2-3 Å from the metal image plane[3]. For the *tilted* phase, the C1s XPS consists of four components with varying screening induced shifts in binding energy due to inequivalent carbon distances from the Au image plane. This spectrum is fit well with two doublets separated by 0.9 eV (light brown and dark brown) corresponding to some carbons that are close to the surface and some that are further away.

The N1s XPS spectra show a single peak for the *multi* and *flat* phase at 399.8 and 399.0 eV respectively (Fig. S1b). The shift between these is consistent with the screening induced shifts seen in the carbon spectra. Furthermore, the single peak seen in the *flat* phase confirms the flat lying BDA molecule has two equivalent nitrogens. In contrast, for the *tilted* phase, two N1s peaks are seen at 399.0 and 399.7 eV, showing that one nitrogen atom is indeed tilted away from the surface.

Near Edge X-Ray Absorption Fine Structure

Near Edge X-Ray Absorption Fine Structure (NEXAFS) measurements were conducted on the carbon and nitrogen K-edges, with incident photon energy varied in steps of 0.1 eV between 280 eV and 310 eV for C and 396 eV and 420 eV for N. The photon incidence angle was set to 6^o. Spectra were acquired using a channeltron detector with a wide acceptance angle in partial electron yield mode, with a high pass filter set to 250 eV (C) or 370 eV (N). The photon flux was monitored on the last optical element along the beam path and a separate measurement of NEXAFS signal was taken on a clean Au substrate for normalization. The sample normal was oriented either parallel to the photon polarization (p-pol) or perpendicular to polarization (s-pol). These measurements were used to determine the orientation of the molecules on the surface (NEXAFS linear dichroism measurement) as follows. In the case of carbon K-edge NEXAFS the intensity of the LUMO (and LUMO+1) absorption peaks at 285 (and 287 eV) in the p-pol (I_p) and s-pol (I_s) measurements are determined. Since LUMO (and LUMO+1) orbitals have a π character oriented perpendicular to aromatic ring, we obtained the average ring inclination θ from the surface as $\theta = \tan^{-1}\sqrt{2I_s/I_p}$ following Reference 4.

Fig. S1c shows carbon NEXAFS spectra for both polarizations for all three surfaces. For multilayer BDA films, we get I_s/I_p=1, consistent with randomly oriented molecules. In the *flat* phase we get a strong NEXAFS dichroism ($I_S \ll I_P$) indicates that the molecules are lying almost perfectly flat. For the tilted phase the I_s/I_p ratio of the LUMO and LUMO+1 transitions yields θ_{tilted}~50°. Fig. S1d shows N K-edge NEXAFS spectra where we see a strong dichroism in the *tilted* phase. This is consistent with the molecular angles found from the carbon NEXAFS, with BDA molecules acquiring *trans* conformation in *tilted* phase with the N lone-pair along the surface normal.

Details of Resonant Photoemission Measurements and Analysis

Resonant photoemission (RPES) at the carbon (nitrogen) K-edge was conducted by taking XPS scans at a series of incident photon energies between 280 eV and 310 eV (397 eV - 420 eV). For each photon energy, XPS spectrum covering 90 eV kinetic energy range was measured to construct a photoemission map as a function of photon energy and electron binding energy. Because of the large energy window, each XPS spectrum contains the whole valence band region as well as the Au $4f_{5/2}$ and Au $4f_{7/2}$ peaks, which serves to calibrate the binding energy (Au $4f_{7/2}$ E_b = 84.0 eV). The non-resonant spectrum was measured in the pre-edge region at a photon energy of 283 eV for carbon and 390 eV for nitrogen. This spectrum was subtracted from each XPS spectrum in the RPES map. For all RPES measurements, incident light was polarized at 54.7^o with respect to the surface normal, which guaranteed the RPES signal independent of molecular orientation.[4] The electron analyzer for RPES was placed at 54.7° from the surface normal and along the photon electric field.

Fig. S4 shows two resonant photoemission spectra of the BDA *multi* and *gas* phase taken at photon energy hν=284 eV and 285 eV corresponding to the absorption from C1s to LUMO and LUMO+1 empty level. High resolution gas phase spectrum measured with photon energy hν =90 eV is also shown together with the vertical bars indicating the DFT calculated energy levels of the BDA occupied states. The photon and kinetic energy dependence of participator intensities in multilayer and in the gas phase spectra are quite similar, which confirms that carbon RPES measurements can be referenced to the *multi* phase for charge transfer time determinations. We notice that strong photoemission resonances occur when there is significant overlap of the empty and filled molecular orbitals over the carbon sites, and are lacking when this overlap is poor. The intensities in the 2D map shown in Fig. S4 reflect calculated Auger matrix elements following equations in References 5 and 6.

In Figure S5, we show the RPES data across the N K-edge for *gas*, *tilted* and *flat* phase used to determine the integrated intensity shown in Figure 4b. We have subtracted, from these data, the non-resonant photoemission spectra at hν < 395 eV. For *gas* phase, we show spectra taken at two energies (401.3 eV and 406.7 eV) as indicated in the inset of Fig. S5a, which highlight the shift of 4-5 eV in the position of the Auger peak as would be expected in an isolated system. In contrast, for the *flat* phase, there is no difference between the Auger spectra at the same two energies, indicating a complete quenching of the spectator Auger signal. In this phase, the participator and spectator intensities associated with the presence of the core excited electron in the LUMO+1 orbital are both completely quenched confirming a charge transfer time below the 500

attoseconds limit of the core-hole clock method. In the *tilted* phase, where one N is bound to the Au substrate and one is unbound, the participator intensity is partly quenched, and the Auger profile at 406.7 eV is slightly shifted compared to that at 401.3 eV. Since the bound N does not contribute to the spectator and participator Auger signal, we can deduce a charge transfer time from the unbound N, as done in the text.

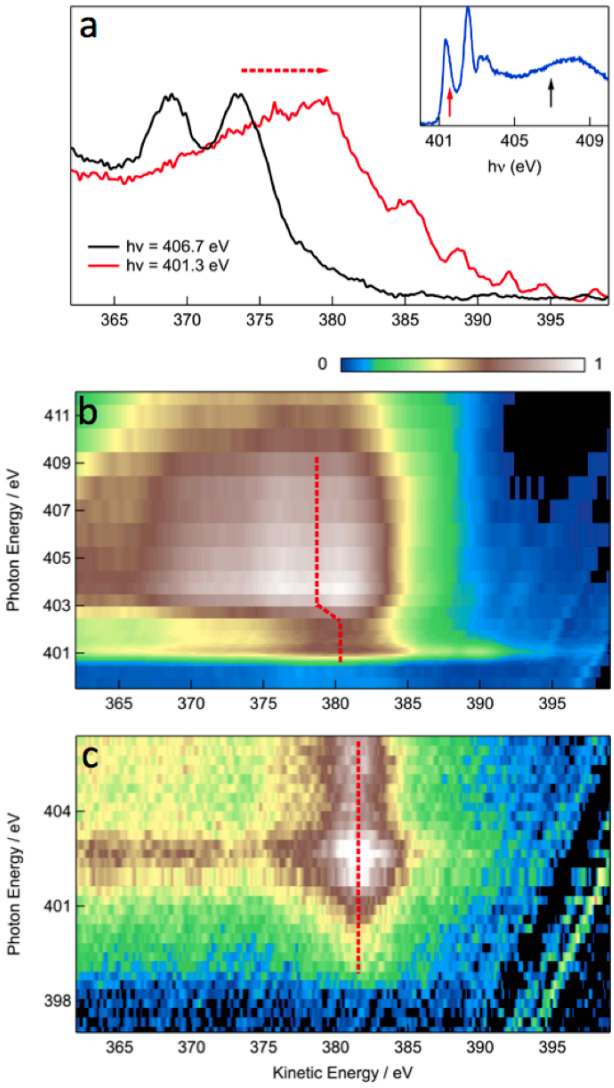

Fig. S5. RPES spectra across the nitrogen K-edge plotted against kinetic energy after the non-resonant contribution measured in the pre-edge section has been subtracted. (a) *Gas* phase: Resonant photoemission spectrum measured on LUMO+1 resonance (red curve) and off resonance (black curve). Inset: nitrogen NEXAFS with two energies indicated. Red dashed arrow indicates the shift in the Auger peak between the two spectra. (b) *Tilted* phase: dashed red line indicates the shift in the Auger peak as a function of photon energy. (c) *Flat* phase: dashed red line marks the position of the Auger peak which does not shift with photon energy.

DFT calculations of molecular orbitals and NEXAFS transitions

We calculate carbon and nitrogen K-edge spectra using GPAW, a grid-based real-space projector-augmented-wave (PAW) code, with the B3LYP exchange-correlation functional[7,8]. For these simulations, isolated molecules were first relaxed to their optimized geometries. Default grid spacings and convergence thresholds were employed. All NEXAFS calculations were performed using the half-core-hole approximation[9]. The absolute energy scale was determined by performing a delta Kohn-Sham calculation and shifting the calculated spectrum using the calculated total energy difference between the ground state and the first core excited state.

References

(1) Floreano, L.; Cossaro, A.; Gotter, R.; Verdini, A.; Bavdek, G.; Evangelista, F.; Ruocco, A.; Morgante, A.; Cvetko, D. Periodic Arrays of Cu-Phthalocyanine Chains on Au(110), *J. Phys. Chem. C* **2008**, *112*, 10794-10802.
(2) Pasquarello, A.; Hybertsen, M. S.; Car, R. Theory of Si 2p Core-Level Shifts at the Si(001)-Sio_{2} Interface, *Phys. Rev. B* **1996**, *53*, 10942-10950.
(3) Smith, N. V.; Chen, C. T.; Weinert, M. Distance of the Image Plane from Metal-Surfaces, *Phys. Rev. B* **1989**, *40*, 7565-7573.
(4) Stohr, J. *Nexafs Spectroscopy*; Heidelberg, 1992.
(5) Bruhwiler, P. A.; Karis, O.; Mårtensson, N. Charge-Transfer Dynamics Studied Using Resonant Core Spectroscopies, *Rev. Mod. Phys.* **2002**, *74*, 703-740.
(6) Föhlisch, A.; Feulner, P.; Hennies, F.; Fink, A.; Menzel, D.; Sanchez-Portal, D.; Echenique, P. M.; Wurth, W. Direct Observation of Electron Dynamics in the Attosecond Domain, *Nature* **2005**, *436*, 373-376.
(7) Enkovaara, J.; Rostgaard, C.; Mortensen, J. J.; Chen, J.; Dulak, M.; Glinsvad, C.; Hansen, H. A.; Larsen, A. H.; Moses, P. G.; Petzold, V.*et al.* Electronic Structure Calculations with Gpaw: A Real-Space Implementation of the Projector Augmented-Wave Method, *J Phys Condens Matter Journal of Physics Condensed Matter* **2010**, *22*.
(8) Ljungberg, M. P.; Mortensen, J. J.; Pettersson, L. G. M. An Implementation of Core Level Spectroscopies in a Real Space Projector Augmented Wave Density Functional Theory Code, *Journal of Electron Spectroscopy and Related Phenomena* **2011**, *184*, 427-439.
(9) Cavalleri, M.; Odelius, M.; Nordlund, D.; Nilsson, A.; Pettersson, L. G. Half or Full Core Hole in Density Functional Theory X-Ray Absorption Spectrum Calculations of Water?, *Physical chemistry chemical physics : PCCP* **2005**, *7*, 2854-2858.